Biomedical Signal Processing and Control 92 (2024) 106105

Contents lists available at ScienceDirect

Biomedical Signal Processing and Control

journal homepage: www.elsevier.com/locate/bspc

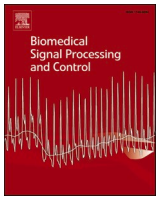

Locomotion transition prediction at Anticipatory Locomotor Adjustment phase with SHAP feature selection

Ziyao Wang [a], Jun Pang [a], Pengyu Tao [b], Zhimin Ji [a], Jingwen Chen [a], Lin Meng [a,*], Rui Xu [a,*], Dong Ming [a]

[a] Academy of Medical Engineering and Translational Medicine, Tianjin University, China
[b] Key Laboratory of Fire Protection Technology for Industry and Public Building, Ministry of Emergency Management, China

ARTICLE INFO

Keywords:
Locomotion recognition
Anticipatory Locomotor Adjustment
Shapley Additive exPlanation
sEMG feature selection

ABSTRACT

Locomotion recognition plays an important role in developing intelligent assistive devices. High accuracy and early prediction in transition recognition are essential for enhancing the performance of these devices. A major challenge faced by previous recognition methods was the lack of timely recognition. In this study, we attempted to address this challenge by employing data from the Anticipatory Locomotor Adjustment phase and applying Shapley Additive exPlanation for feature selection. We recruited ten healthy participants and collected their sEMG and kinematic signals while they performed various locomotion modes, including 3 steady-state modes and 4 transition modes. Features were extracted from three gait phases: FC 0 (the foot contact immediately preceding transition onset), SW −1 (the mid-swing immediately preceding FC 0), and FC −1 (the foot contact immediately preceding FC 0) during the Anticipatory Locomotor Adjustment phase. In preliminary validation, the recognition accuracy of 7 modes based on FC 0 data reached 97%. In sEMG feature selection, it was found that RMS was the most effective feature and adding sEMG features with lower SHAP values did not significantly improve the recognition accuracy. In channel selection, the recognition accuracy achieved 95% with 12 channel inputs (the baseline classification strategy) and with 6 channel inputs (the mode-specific classification strategy). With the same methods, the recognition accuracy based on SW −1 and FC −1 data were both above 95%. In conclusion, our proposed method made two optimizations to ensure timely recognition of locomotion and achieved an early and accurate prediction of locomotion. This study provides a promising application prospect for further development of intelligent assistive devices.

1. Introduction

The recognition of human activities is crucial for the development of intelligent robots that can assist humans in completing tasks more efficiently [1,2]. In healthcare, recognizing locomotion patterns is a key step towards developing intelligent assistive devices that can effectively support individuals in living independently [3]. This is particularly important for walking on level ground and stairs. Compared to level-ground walking, stair ascent and descent require greater physical strength and can pose significant challenges for elderly or disabled individuals [4]. To provide better support for those with mobility difficulties, intelligent assistive devices must be able to recognize different lower-limb locomotion modes corresponding to different terrains and provide tailored assistance accordingly.

Advances in sensor technology have led to the extensive use of wearable devices that collect electrophysiological, mechanical and kinematic data for locomotion recognition [5–7]. Locomotion recognition typically employs machine learning to classify the data collected from wearable devices. Huang et al. [8] achieved an accuracy of over 90 % in recognizing user locomotion modes through phase-dependent classification based on surface electromyographic (sEMG) signals. Martinez et al. [9] presented an approach for recognizing lower-limb locomotion modes and gait events based on angular velocity signals obtained from inertia measurement units (IMUs), achieving accuracy of 99.87 % and 99.82 %, respectively. In order to improve the accuracy of locomotion recognition, data fusion has been adopted commonly. The effectiveness of various feature combinations has been demonstrated in previous studies [10–15]. Such combinations included sEMG signals with prosthetic mechanical signals [10], sEMG signals with IMU signals [11], and sEMG signals and electroencephalogram (EEG) signals [12]. These

* Corresponding authors.
E-mail addresses: linmeng@tju.edu.cn (L. Meng), xrblue@tju.edu.cn (R. Xu).

https://doi.org/10.1016/j.bspc.2024.106105
Received 24 October 2023; Received in revised form 22 January 2024; Accepted 9 February 2024
Available online 13 February 2024

studies demonstrated the feasibility of the lower-limb locomotion mode recognition with multi-types of wearable sensors.

Locomotion recognition with steady-state data has achieved a high accuracy. However, the key process for controlling intelligent assistive devices according to demand is the locomotion transition recognition [16,17]. Previous studies [18–23] have improved the recognition methods for lower-limb locomotion and its transitions. Spanias et al. [20] developed and evaluated an adaptive recognition algorithm based on sEMG and mechanical signals, achieving an accuracy of over 96 % for locomotion transition recognition. Lee et al. [22] developed a recognition framework based on sEMG and kinematic signals that implemented convolutional neural networks with image encoding, and obtained an accuracy of 94.55 % for locomotion transition recognition. These studies have achieved some success in locomotion transition recognition, but there are still challenges to be addressed.

The first problem is that most studies recognized steady-state modes and transition modes separately. This method relies a priori knowledge of the locomotion states, which is untenable in practical applications. Furthermore, transition modes should be labeled based on the two types of locomotion that precede and follow the transition. This is essential, as similar transitions exhibit noteworthy kinematic differences [24–26]. Therefore, Su et al. [21] labeled each locomotion transition mode and simultaneously recognized both steady-state modes and transition modes. Young et al. [19] developed a mode-specific classification strategy that recognized each locomotion mode based on previous locomotion mode. These studies provided effective classification strategies for transition recognition.

The timeliness of recognition, recognizing early enough for decision-making, is another major challenge for locomotion transition recognition. Ideally, the classifier should accurately predict the locomotion transition before it occurs. If the recognition is completed after the onset of locomotion transition, there is a lack of specific support from assistive devices at the early phase of the locomotion transition. Therefore, some studies [27–29] tried to predict locomotion before it actually happened. In these studies, the model was trained exclusively on steady-state locomotion data, while locomotion transition data was introduced during testing as novel input for transition prediction. The transition recognition moment was defined as the first correct recognition of locomotion following a transition. However, the recognition based on this method still occurred later than the onset of transition.

In biomechanical research, it has been demonstrated that people make a series of anticipatory adjustments upon detecting obstacles in their path [30]. This strategy is known as Anticipatory Locomotor Adjustments (ALA). Previous studies have demonstrated significant differences in kinematic and sEMG data between the transition from walking to stair ascent/descent and the steady-state walking during ALA phase [31]. These findings suggested the potential utility of ALA phase data for transition prediction.

To ensure timely recognition, it is also crucial to optimize the computational efficiency of classifiers. The classification features have a direct impact on the computational efficiency, which can be decreased by redundant features [32]. Therefore, feature selection is an important step for recognition. Previous studies [11,22,23] explored the impact of various feature inputs for locomotion recognition. However, a definitive consensus on the optimal set of features remains elusive and the 'black box' nature of machine learning models is a significant challenge to feature selection. Shapley Additive exPlanations (SHAP) is an explainable machine learning algorithm that employs a game-theoretic approach to explain the output of any machine learning model [33]. It provides a powerful tool for understanding complex algorithms and is currently one of the most popular methods in explainable machine learning [34–36]. Recently, SHAP was employed for feature selection [37–39]. Gozzi et al. [37] adapted SHAP to evaluate the contribution of EMG features in feature selection for hand gesture classification. Liu et al [38] demonstrated that SHAP outperformed other methods for feature selection in Parkinson's disease diagnosis. Consequently, employing SHAP for feature selection can result in an optimal input dimensionality and an improved computational efficiency for transition prediction.

In this study, we focused on the timely and accurate recognition of locomotion transition. ALA mechanism and SHAP algorithm were employed to optimize data source and computational efficiency for this challenge. The detailed work of this study were:

1. to verify the feasibility of locomotion transition recognition with ALA phase data in a timely and accurate way;
2. to determine the most effective features for locomotion transition recognition based on SHAP analysis;
3. to evaluate the effectiveness of this method with data from different periods during the ALA phase.

2. Methods

2.1. Participants and measurements

In this study, we recruited 10 healthy participants (5 females and 5 males; mean age: 22.9 ± 0.57 years; mean weight: 62.5 ± 11.5 kg; mean height: 169.3 ± 7.96 cm) without orthopedic or neurological pathologies. The sEMG data were collected from fourteen sites on both legs with sEMG collectors (Noraxon, USA). The sites included the position of the rectus femoris (RF), vastus lateralis (VL), semitendinosus (SEM), biceps femoris (BF), tibialis anterior (TA), gastrocnemius lateralis (GASL), and gastrocnemius medialis (GASM) for both legs. Additionally, the 3-axis angular velocity signals were obtained by four IMUs (Noraxon, USA) on bilateral thighs and shanks. Both sEMG and IMU data were sampled at a rate of 2000 Hz, with sEMG signals filtered between 10 and 500 Hz by the hardware. Four reflective spherical markers were attached to bilateral heels and toes of each participant. Gait events were detected based on the location of the markers collected at 100 Hz with a motion capture system (Vicon, UK). The Experiment setup for data collection is illustrated in Fig. 1. All data were recorded synchronously.

2.2. Experimental protocol

In the experiment, each participant was required to complete seven locomotion modes: level-ground walking (W), stair ascent (SA), and stair descent (SD) for steady-state modes; and level-ground walking to stair ascent (W-SA), level-ground walking to stair descent (W-SD), stair ascent to level-ground walking (SA-W), and stair descent to level-ground walking (SD-W) for transition modes. The schematic diagram of experimental platform is illustrated in Fig. 2(a). During the experiment, the participants were instructed to walk at a self-selected pace while wearing walking shoes. The sequence of tasks for each participant was randomly determined. In an instance of the sequence, the participants

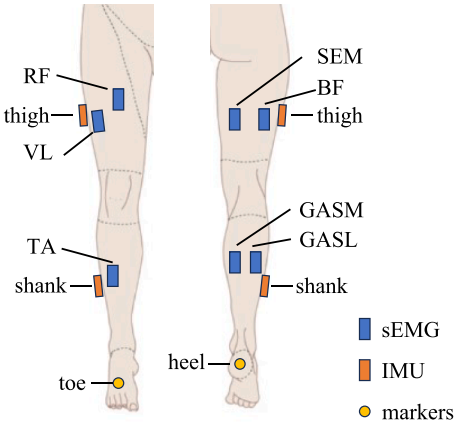

Fig. 1. Experimental setup for data collection.

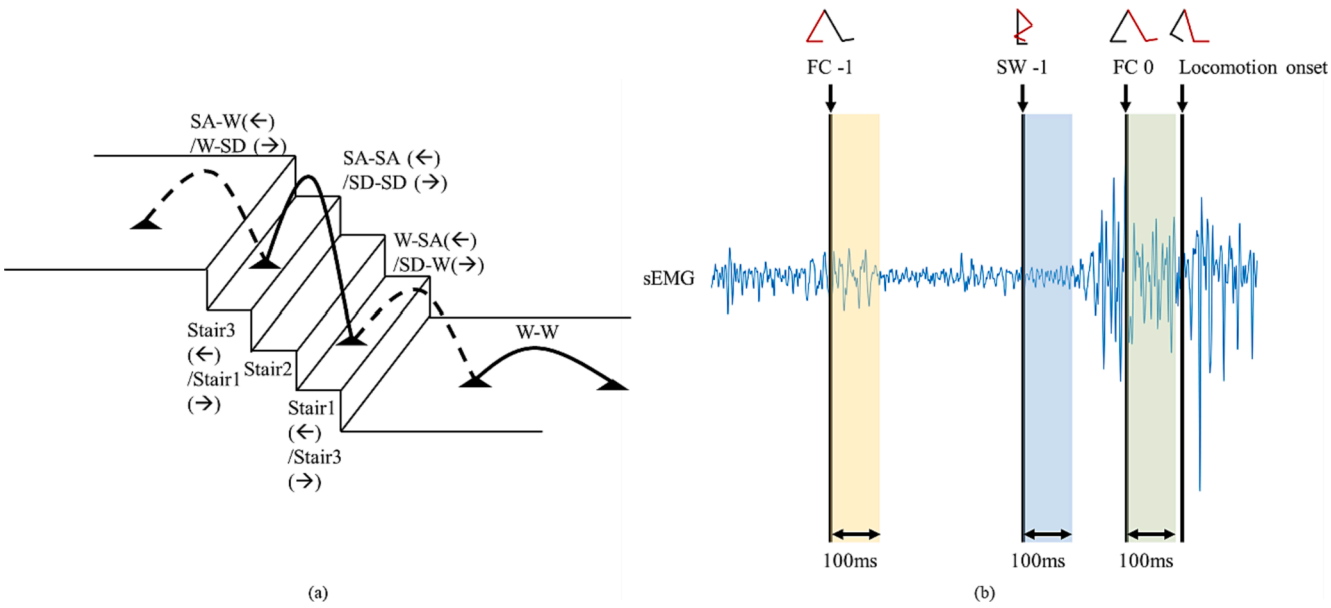

Fig. 2. Experimental set-up (a) and data window definition (b). The dashed line indicates a transition step, while the solid line indicates a steady-state step in (a). W-W: level-ground walking to level-ground walking; W-SA: level-ground walking to stair ascent; W-SD: level-ground walking to stair descent; SA-SA: stair ascent to stair ascent; SA-W: stair ascent to level-ground walking; SD-SD: stair descent to stair descent; SD-W: stair descent to level-ground walking.

completed the first task with steady-state walking on level ground. During the subsequent task, they walked to the stairs, ascended the stairs in a step-over-step gait, walked forward on an elevated platform at the top of the stairs before stopping and turned around. In the final task, the participants walked forward again and descended the stairs in a step-over-step gait before continuing to walk on level ground. The participants were required to complete at least twenty rounds, each of which included all seven locomotion modes. To mitigate the effects of muscle fatigue, the participants were provided with rest breaks between rounds. The experiment protocol was approved by the ethics committee of Tianjin University and all participants provided informed consent prior to participation.

2.3. Data processing

The data were labeled with the locomotion modes for classification. In this study, we followed the naming rules used by Su et al. [21] to label each transition mode. The steady-state mode was considered as a special transition mode during which the locomotion remained the same. For consistency in naming, these locomotion modes were defined as W-W, SA-SA, SD-SD, W-SA, W-SD, SA-W and SD-W. The locomotion modes are illustrated in Fig. 2(a). The W-W step was a step that started with the foot-off on level ground and ended with the next foot-strike on level ground. Similarly, the SA-SA or SD-SD step began with the foot-off on a stair and continued until the next foot-strike on a stair. More importantly, we defined the transition step as a step beginning with the foot off terrain A and ending with the same foot striking on terrain B. Specifically, the W-SA or W-SD transition step began with the foot off the level-ground and ended with the same foot striking on the stair (stair1 in Fig. 2(a)), and the SA-W or SD-W transition step began with the foot off the stair (stair3 in Fig. 2(a)) and ended with the same foot striking on the level-ground.

In this study, we define the ALA phase of interest based on the swing leg during the transition step. Specifically, the ALA phase was the stance phase of the swing leg preceding transition step. This ALA phase occurred prior to the onset of the transition step and consisted of two double stance phases and one swing phase. The sEMG and angular velocity data were collected from three 100-ms windows, chosen not to exceed the duration of the double stance phase, i.e. the 100-ms data collected at the two double stance phases and the middle swing phase in between (Fig. 2(b)). Twenty data windows were collected for each phase. The data window of double stance phase temporally proximal to transition step onset, was referred to as FC 0 (foot contact). The remaining two data windows were respectively referred to as SW −1 (swing) and FC −1. The 14 different features (Table 1), selected based on previous research [37,40,41], were extracted from the filtered sEMG as

Table 1
Features extracted from sEMG.

Feature name	Formula
Root Mean Square (RMS)	$RMS = \sqrt{\frac{1}{N}\sum_{i=1}^{N} x_i^2}$ (2)
Waveform Length (WL)	$WL = \sum_{i=1}^{N-1} \lvert x_{i+1} - x_i \rvert$ (3)
Mean Average Value (MAV)	$MAV = \frac{1}{N}\sum_{i=1}^{N} \lvert x_i \rvert$ (4)
Zero Crossing (ZC)	$ZC = \sum_{i=1}^{N-1} \begin{bmatrix} sgn(x_i \times x_{i+1}) \cap \\ \lvert x_i - x_{i+1} \rvert \geq threshold \end{bmatrix}$ (5)
Slope Sign Change (SSC)	$SSC = \sum_{i=1}^{N-1} \{f[(x_i - x_{i-1}) \times (x_i - x_{i+1})]\}$ (6) $f(x) = \begin{cases} 1, if x \geq threshold \\ 0, otherwise \end{cases}$
Hjorth Parameter (HP)	Hjorth Parameter Activity (HPA): $HPA = \frac{1}{N}\sum_{i=1}^{N} \lvert x_{i+1} - \bar{x} \rvert$ (7) Hjorth Parameter Mobility (HPM): $HPM = \sqrt{\frac{HPA(x_i')}{HPA(x_i)}}$ (8) Hjorth Parameter Complexity (HPC): $HPC = \frac{HPM(x_i')}{HPM(x_i)}$ (9)
Auto-regressive (AR)	$x_i = c + \sum_{p=1}^{P} AR_p x_{i-p} + w_i$ (10) c is a constant; W_i is white noise1; P is the order of the AR model. The fourth-order AR was suggested from previous research works. Our study also employs a fourth-order AR model.
Sample Entropy (SE)	$SE = -ln\frac{A^{m+1}(r)}{A^m(r)}$ (11) m is the embedding dimension, representing the length of the constructed vectors; r is the similarity threshold; A^m represents the probability that template vectors of length m have a distance less than r
Skewness (SKEW)	$SKEW = \frac{1}{N}\sum_{i=1}^{N} \left(\frac{\lvert x_{i+1} - \bar{x} \rvert}{\sigma}\right)^3$ (12) σ is the standard deviation

the sEMG features. The mean angular velocity was extracted as the kinematic feature. Each feature was considered an independent channel, providing unique information for recognition. The data during FC 0 were used to verify the feasibility of transition prediction and complete feature selection. During the verification process, a combination of RMS (a commonly-used sEMG feature) and the kinematic feature were employed as input. Our findings were subsequently tested with data during the remaining two data windows.

2.4. Feature selection

Feature selection included sEMG feature selection and channel selection, determining the optimal method for extracting valuable information hidden in sEMG and identifying informative channel for locomotion recognition. Feature selection was performed based on SHAP values. SHAP calculates the contribution of each feature to the classifier's output by employing Shapley values from coalitional game theory to elucidate the principles of the classifier. Specifically, for a given input instance x and model f_x, the Shapley value for feature x_j can be defined as:

$$\phi_j = \sum_{S \subseteq x_1, \cdots, x_n \backslash x_j} \frac{|S|!(n - |S| - 1)!}{n!} \left[f_x(S \cup x_j) - f_x(S) \right] \quad (1)$$

where $x_1, \cdots, x_n$ is the set of all features, n is the total number of features, $x_1, \cdots, x_n \backslash x_j$ is the set of all features excluding x_j, S is any subset in $x_1, \cdots, x_n \backslash x_j$, $|S|$ is the number of features in S, and $f_x(S)$ is the output of model f_x with S as the input. This formula determines the contribution of feature x_j to the output by considering all possible coalitions. Specifically, it calculates how much adding feature x_j changes the output with S as the input. The feature contribution to the classifier's output is shown by the Shapley value. However, calculating exact Shapley values can be computationally challenging due to the large number of subsets that must be considered. In this study, Kernel SHAP was employed to approximate Shapley values. This method addresses the computational challenge by estimating the contributions of each feature through a weighted linear regression [33,42].

In the selection of sEMG feature, correlation coefficients between each feature were calculated. Features with a correlation coefficient exceeding 0.9 were removed until all remaining features had a correlation coefficient lower than 0.9. This process reduced redundant features to decrease the bias in the training model and the computational cost in SHAP. The non-correlated features retained included Root Mean Square (RMS), Zero Crossing (ZC), Slope Sign Change (SSC), Hjorth Parameter Mobility (HP_M), Hjorth Parameter Complexity (HP_C), the third autoregressive coefficient (AR-3), Sample Entropy (SE) and Skewness (SKEW). The selection of sEMG feature was conducted with both combined input (sEMG and kinematic features) and sEMG input only. The non-correlated features were employed as input to train the model, and the SHAP values of each input were calculated. The SHAP value of the sEMG feature was determined by summing its SHAP values across all muscles and the mean SHAP values were calculated for all trial of each participant. To analyze the mean SHAP values for each sEMG feature, a two-way repeated measures analysis of variance (RMANOVA) was conducted. The factors included non-correlated sEMG feature and whether adding the kinematic feature or not. Based on the analysis, the sEMG feature input was divided into different sEMG feature sets. The impact of different sEMG feature sets on classification accuracy was compared based on a two-way RMANOVA. The factors included sEMG feature sets and whether adding the kinematic feature or not.

Channel selection was completed based on the result of sEMG feature selection. The optimal sEMG feature set and kinematic feature were employed as fusion features to input into the classifier, and the SHAP values of 26 channels, including 14 sEMG channels and 12 angular velocity channels, were calculated. According to the ranking of SHAP values, the inputs from the top 1 to top 26 channels were evaluated according to their recognition accuracy.

2.5. Classification strategies

In this study, Support Vector Machines (SVMs) were employed due to their effectiveness in situations with limited training data. To better leverage the contribution of each channel, both the baseline classification strategy and the mode-specific classification strategy proposed by Young et al. [19] were tested. The processes of these two strategies are illustrated in Fig. 3. The baseline classification strategy directly output seven types of locomotion through a single classifier. The mode-specific classification strategy employed a hierarchical classification approach, utilizing a first-layer classifier and three second-layer classifiers to achieve accurate classification. A 10-fold cross-validation was used to evaluate the classification results for each participant.

3. Results

3.1. Feasibility of recognition with ALA phase data

Fig. 4 shows the classification performance with ALA phase data from FC 0. The recognition accuracy reached 97.00 %±3.23 %, based on the combined input (RMS and kinematic features) and the baseline classification strategy. The confusion matrix in Fig. 4 illustrates the percentage of each actual locomotion (vertical axis) corresponding to

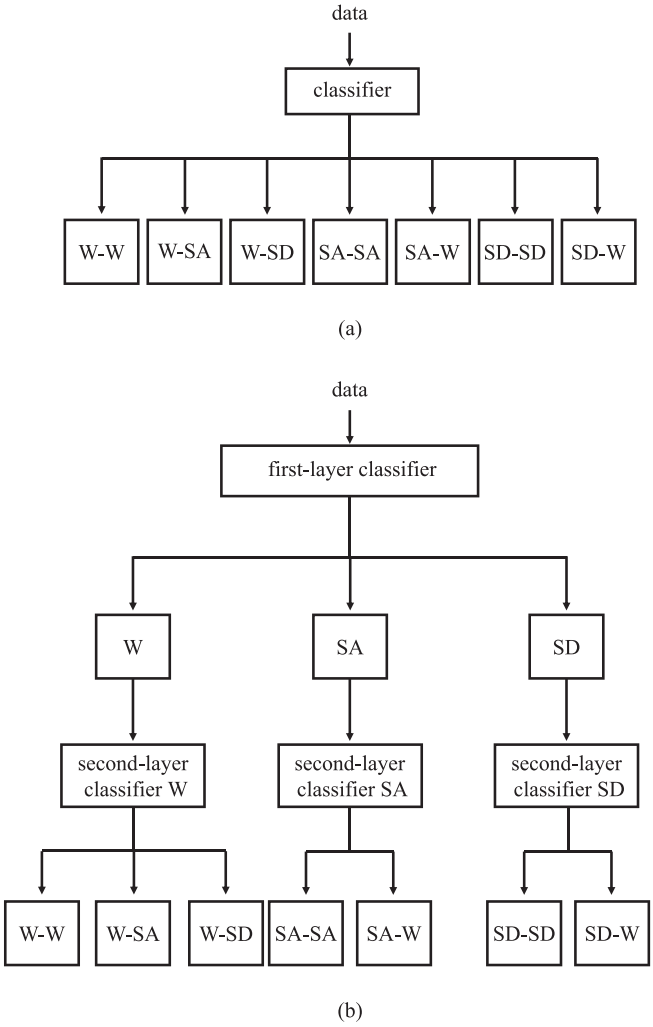

Fig. 3. Schematic diagrams of both classification strategies. (a). The baseline classification strategy. (b) The mode-specific classification strategy.

Fig. 4. Confusion matrix of classification with ALA phase data at FC 0.

the prediction (horizontal axis). The average recognition accuracy for each locomotion was no less than 96 %, with outstanding performance for both steady-state modes and transition modes.

3.2. Effect of sEMG features

Fig. 5 shows the SHAP values for each non– correlated sEMG feature with the baseline classification strategy based on both combined input (sEMG and kinematic features) and sEMG input only, respectively. Box plots in Fig. 5(a) and Fig. 5(b) illustrate the mean SHAP for all participants. In Fig. 5(c) and Fig. 5(d), the SHAP values are displayed for each trial of the ten participants, totaling 1400 trials.

Preliminary results of the two-way RMANOVA indicated a significant main effect of the sEMG feature ($p < 0.001$) and a significant interaction ($p < 0.001$). The simple effect analyses revealed significant differences between mean SHAP values of sEMG features (combined input $p < 0.001$, sEMG input only $p < 0.001$). With combined input, significant differences were found between all pairs except RMS & ZC, ZC & SSC, and HP_C & SKEW. With only sEMG input, significant differences were found between all pairs except ZC & SSC, and HP_C & SKEW. The mean SHAP values for RMS, ZC and SSC were significantly greater than those for other features, with the largest mean SHAP value for RMS. The mean SHAP values for SE and HP_M were significantly greater than those for HP_C SKEW and AR_3. The trends observed in SHAP values were consistent with the results of the mean SHAP values. Based on the result of the SHAP values for non-correlated sEMG feature, we divided the sEMG features into five sEMG feature sets (Table 2).

Fig. 6 shows the classification performance with various sEMG feature sets based on the baseline classification strategy. RMS was found to be the best sEMG feature set for the classification with the combined input (97.00 %±3.23 %), while Top 5 was found to be the best sEMG feature set for the classification with only sEMG features (90.64 %±5.29 %).

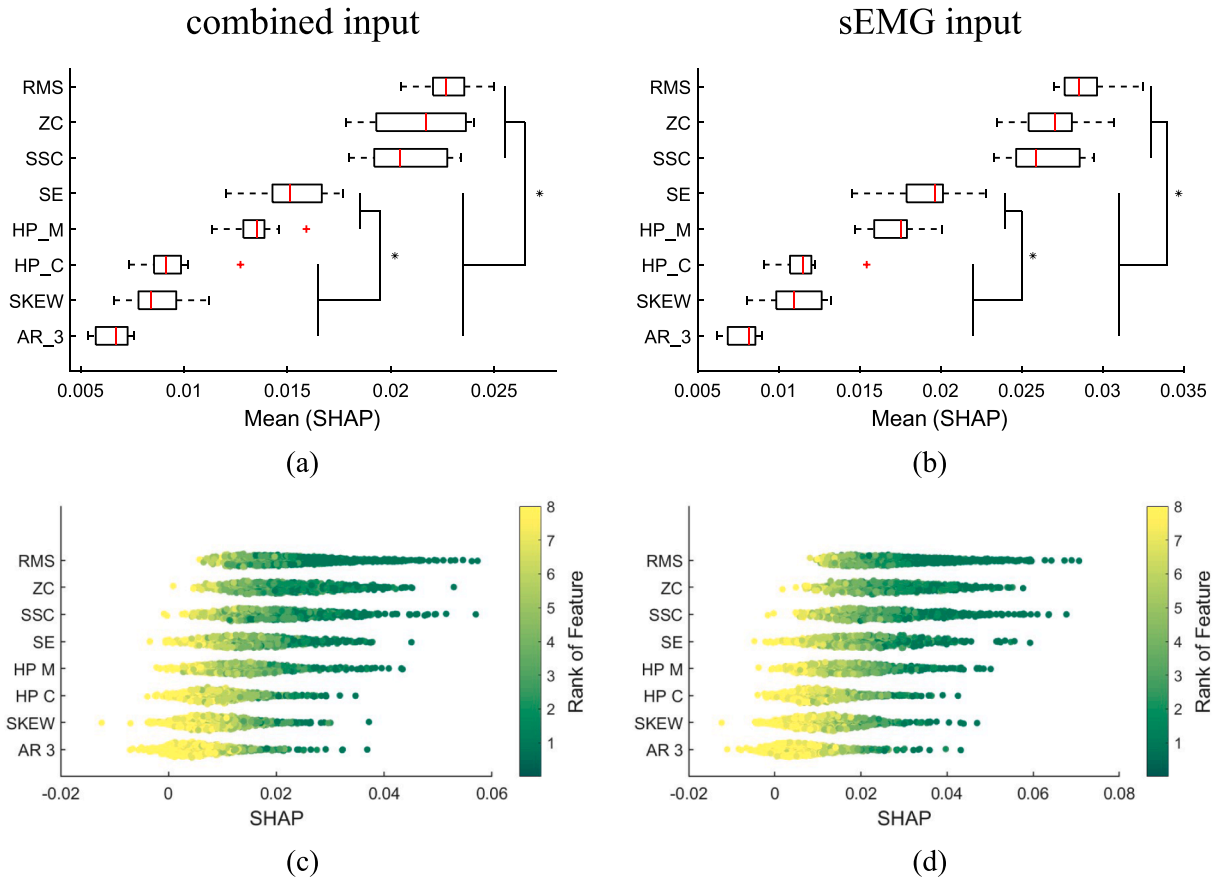

Fig. 5. SHAP values for each non-correlated sEMG feature during classification. (a)&(b) The mean SHAP values for all participants. (c)&(d) The SHAP values for each trial of the ten participants. (a)&(c) combined input. (b)&(d) sEMG input. The sEMG features were sorted in a descending order based on the median of the mean SHAP values for all ten participants. The SHAP values are color-coded based on their SHAP value ranking in a single trial. '*' indicates significant differences ($p < 0.05$).

Table 2
Five feature sets for sEMG features.

Feature set name	Features included in the set
RMS	RMS
Top 3	RMS, ZC and SSC
Top 5	RMS, ZC, SSC, HPM and SE
Non-correlated	All 8 Non-correlated features
Full	All 14 sEMG features

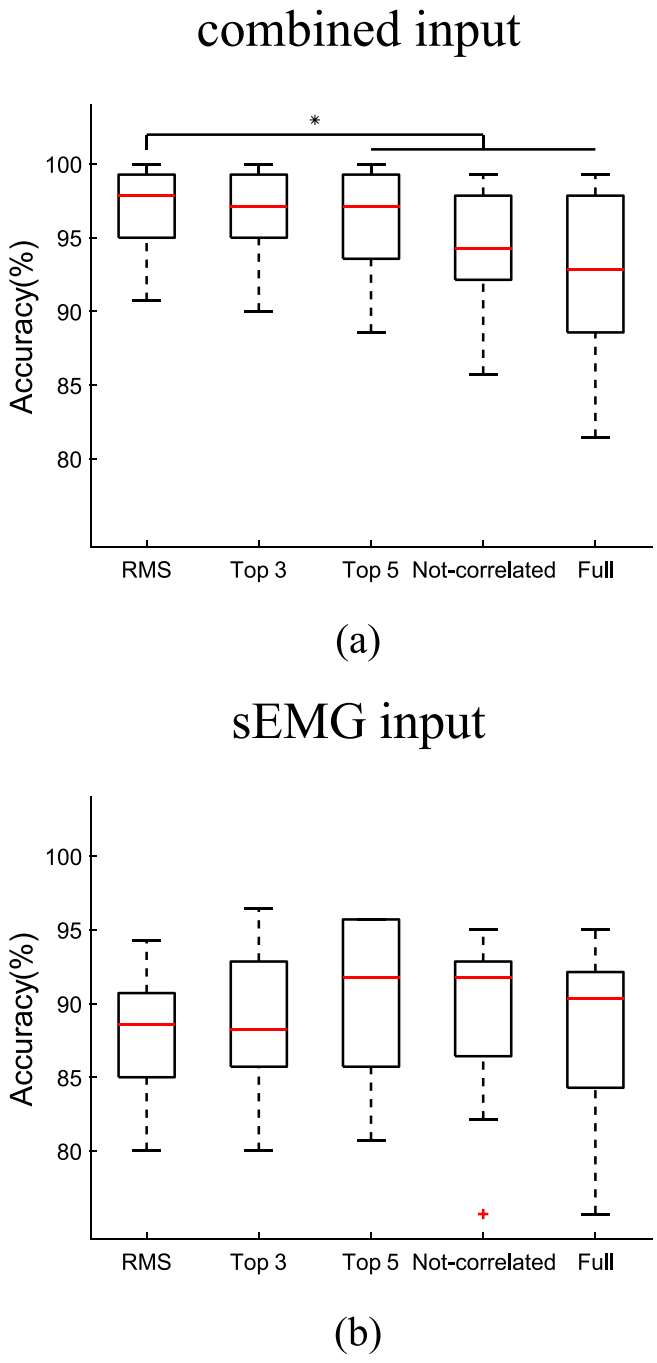

Fig. 6. Recognition accuracy with various sEMG feature sets. (a) The combined input (sEMG and kinematic features) (b) The sEMG input only '*' indicates significant differences ($p < 0.05$).

Preliminary results of the two-way RMANOVA indicated a significant main effect of the sEMG feature set ($p = 0.032$) and a significant interaction effect ($p < 0.001$). With combined input, the simple effect analysis revealed a significant difference between the accuracy of sEMG features sets ($p = 0.005$). Further pairwise comparisons showed that RMS was significantly superior to other sEMG feature sets except Top 3. However, there was no significant difference between accuracy of sEMG feature sets with only sEMG input. Based on the result of the accuracy for various sEMG feature sets, subsequent work would employ RMS as the sEMG feature.

3.3. Effect of channel input

Fig. 7 shows the SHAP values for channels during various locomotion modes. This result demonstrated that the SHAP values were influenced by both the participants and the type of locomotion. For example, sEMG for the L RF was an important channel in participant 1 and 3 but not in participant 2. Furthermore, it was far more important in recognizing SD-W within participant 1 compared to recognizing other locomotion modes.

Fig. 8 shows the classification performance with different numbers of channel inputs. Channels were sequentially input into the classifier in the descending order of their SHAP values. The baseline classification strategy with 21 channels as input achieved the best recognition accuracy of 97.29 % ± 2.54 %. The mode-specific classification strategy with 16 channels as input achieved the best recognition accuracy of 97.86 % ± 2.13 %. Furthermore, both classification strategies achieved a recognition accuracy of 95.21 % with 12 and 6 channel inputs respectively.

3.4. Evaluation with different time windows

Fig. 9 shows classification performance with different numbers of channel inputs based on data from different time windows during the ALA phase. The best recognition accuracy reached 95.64 % ± 3.66 % and 96.14 % ± 2.92 % with 10 channels for SW −1 and 16 channels for FC −1, respectively. Furthermore, data from SW −1 and data from FC −1 achieved recognition accuracy of 95 % with input of 9 and 8 channels (95.00 % and 95.29 %), respectively. These results demonstrated that our approach can accurately recognize various locomotion modes at different time during the ALA phase.

4. Discussion

Accurate and timely recognition of locomotion is crucial for intelligent assistive devices. In this study, we improved the recognition method for both steady-state modes and transition modes with the classification strategy proposed in previous studies [19,21]. Our improvements primarily focused on employing biomechanical theory and explainable machine learning method to optimize the data source and enhance computational efficiency for locomotion prediction. Inspired by biomechanical studies of gait analysis, we proposed a novel locomotion prediction method based on data during the ALA phase, which occurred prior to the actual movement and varied with different movement patterns. Furthermore, we analyzed the impact of various sEMG features and input channels on classification through SHAP analysis and improved our recognition efficiency based on these findings. These works can ensure the accuracy and timeliness of transition recognition, optimizing the functionality and effectiveness of intelligent assistive devices.

4.1. Anticipatory Locomotor Adjustment

Peng et al. [31] conducted a detailed analysis of how humans adjusted their biomechanics in anticipation of transitions from level-ground walking to stair ascent/descent. Significant changes in both

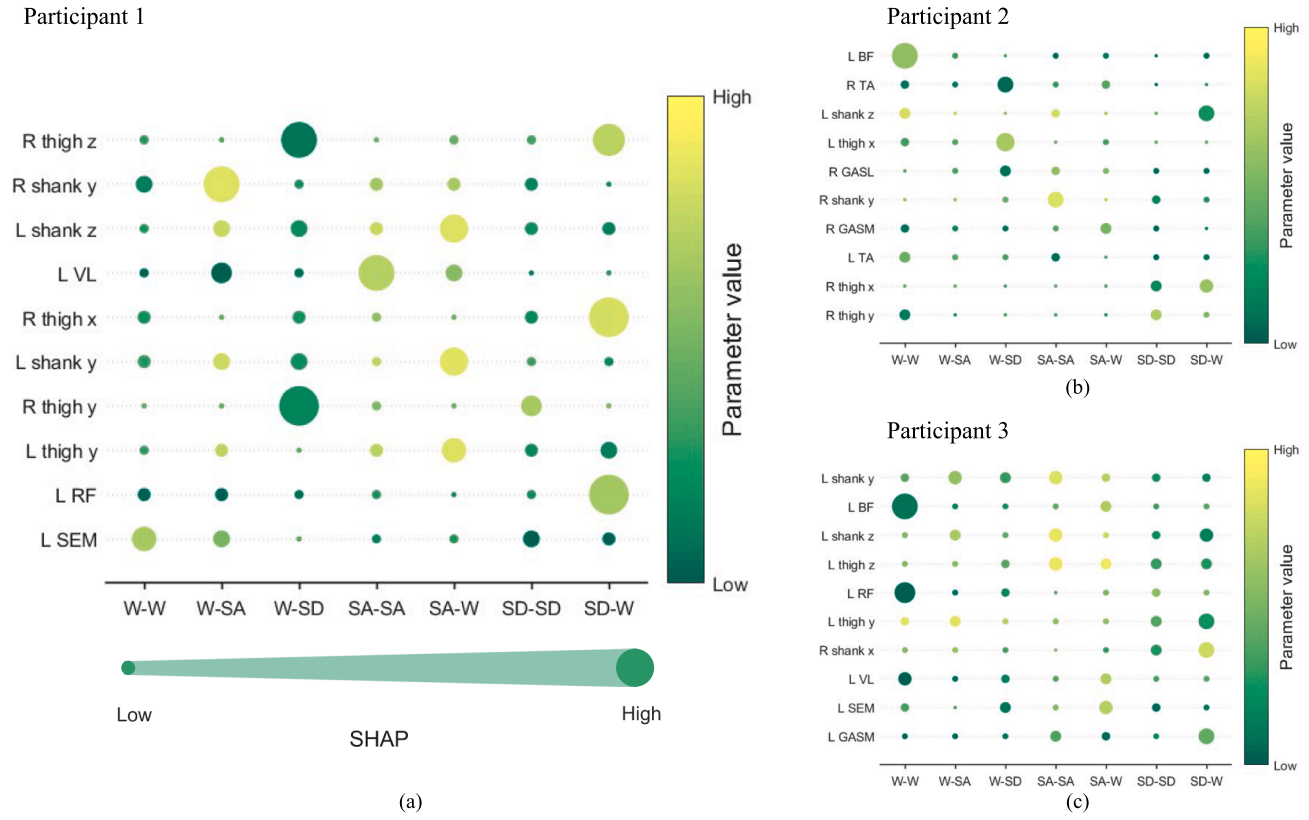

Fig. 7. The SHAP values for channels from three participants during various locomotion modes. Only the 10 highest-ranking channels of the mean SHAP are displayed in descending order. The SHAP value is represented through the size of the corresponding visual elements, and these elements are color-coded to reflect the parameter value. L/R: left/right leg; x/y/z: x/y/z axis of IMUs.

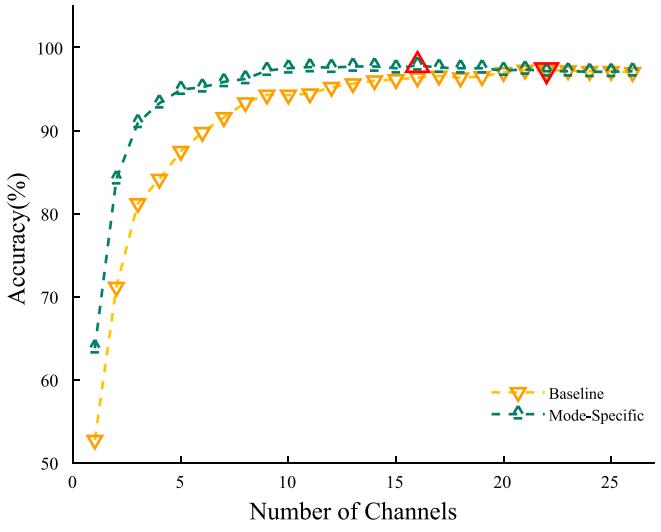

Fig. 8. The recognition accuracy with different numbers of channel inputs based on the baseline classification strategy (yellow inverted triangles) and the mode-specific classification strategy (green triangles). A red outline indicates the least channel number required for achieving the highest recognition accuracy.

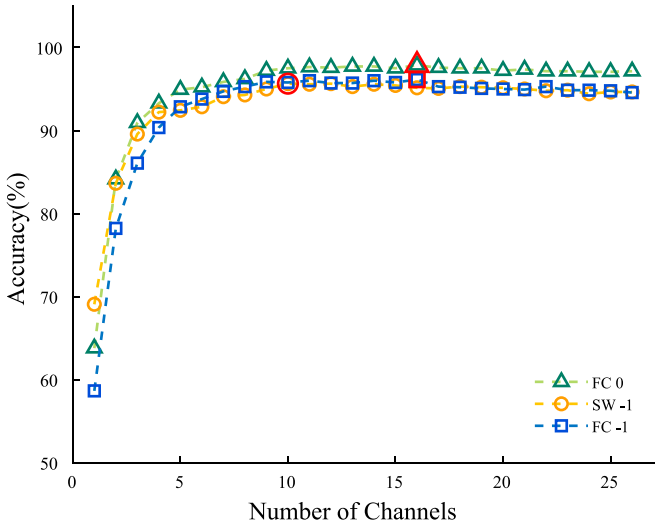

Fig. 9. The recognition accuracy with different numbers of channel inputs based on data from different data windows (FC 0: green triangle; SW −1: yellow circle; FC −1: blue square). A red outline indicates the least channel numbers for achieving the highest recognition accuracy.

kinematic and sEMG features were observed during the ALA phase between the transition mode (W-SA/W-SD) and the steady-state mode (W-W). For example, the tibialis anterior activity of the trailing leg decreased during the terminal swing phase prior to W-SD compared to W-W. In our data, we observed a similar trend based on the mean RMS of TA during the FC 0 phase. Inspired by these results, we verified the feasibility of locomotion recognition with ALA phase data, achieving recognition accuracy above 95 % (FC 0: 97.86 % ± 2.13 %, SW −1: 95.64 % ± 3.66 %, FC −1: 96.14 % ± 2.92 %).

Traditional recognition studies [27–29] usually established classifiers based on steady-state locomotion data to predict locomotion transitions. This approach constrained the transition recognition moment not to precede the onset of the transition. Consulting some

previous biomechanical studies, our approach that recognized locomotion with ALA phase data overcame the limitation of traditional approaches and improved assistive devices to receive accurate instructions before the onset of the transition.

4.2. Shapley Additive exPlanation

An important application of SHAP is feature selection based on feature contribution. Liu et al. [38] conducted feature selection in a Parkinson's disease diagnosis study and demonstrated that SHAP outperformed traditional feature selection methods, including F-score, ANOVA F, and mutual information, in terms of classification accuracy. Therefore, SHAP was employed to select sEMG features and input channels.

4.2.1. sEMG feature selection

Two different input modes, combined input (sEMG and kinematic features) and sEMG input only, were considered for sEMG feature selection in our study. The results of the SHAP analysis, which ranks the importance of various sEMG features, remains a consistent trend across two different input modes. RMS, ZC and SSC, three simple time-domain features, were found to be the most effective. However, ZC and SSC were considered unimportant by Gozzi et al. [37], which may be due to different thresholds in feature calculation formulas. In our study, a threshold condition was applied to avoid low voltage fluctuations or background noise, resulting in a high correlation between ZC, SSC and RMS.

Further, based on the SHAP analysis, we established five sEMG feature sets to evaluate the impact of the adding features with lower SHAP values on locomotion recognition accuracy. The results showed that the feature adding did not significantly improve the recognition accuracy. Additionally, classifiers with fewer features exhibited improved response speed. Therefore, our subsequent work adopted RMS as the sEMG feature, and it was identified as the optimal method that extracts valuable information hidden in the sEMG signals. Our results are consistent with the result of Gozzi et al. in gesture classification with sEMG input only. They found that employing three optimal sEMG features (RMS, HPM, HPC), as determined by SHAP, achieved performance comparable to employing all features ($p > 0.05$) and resulted in a reduction in computational time [37]. These outcomes serve to reinforce and substantiate our findings.

4.2.2. Channel selection

The importance of each channel input was calculated based on SHAP values and the recognition accuracy was tested by sequentially increasing channels in SHAP-descending order. Fig. 7 showed that the participant and the type of locomotion had impacts on the SHAP values of channels. Therefore, we introduced the mode-specific classification strategy that simplified the seven-class problem into several three/two-class problems. Essentially, this strategy is a recommended hierarchical classification strategy [15], without relying on prior knowledge of the previous step.

The optimal number of channels for the mode-specific classification strategy was determined based on the final classification recognition accuracy, since it is difficult to unify the criteria for determining the optimal channel number in each classifier layer. Ultimately, the mode-specific classification strategy achieved a recognition accuracy of 95.21 % with 6 channel inputs and reached its optimal recognition accuracy of 97.86 % with 16 channel inputs. This demonstrated the potential for high accuracy even with limited data input. Since the importance ranking of channels in each layer of classification was different, this method can optimize the computational efficiency for classification but may not reduce the sensors required for actual collection. The results of channel selection for the baseline classification strategy can be referred to reduce the number of sensors required for actual data collection. It achieved a recognition accuracy of 95.21 % with 12 channel inputs and reached its optimal recognition accuracy of 97.29 % with 21 channel inputs. These findings demonstrated that appropriate reduction of channels can optimize the locomotion recognition.

5. Comparation and Limitations

Table 3 presents a comparison of our method with the state-of-the-art methods in the field of locomotion recognition. With 6 channels for predicting 3 steady state modes and 4 transition modes, our method achieved a recognition accuracy of 95.21 %. Compared to previous methods, our method employed a similar number of channel inputs and predicted more challenging transitions [14]. Furthermore, it achieved a recognition accuracy comparable to other methods. Although this classification method shows great potential for locomotion transition prediction, several limitations are present in the study. Firstly, data was only collected from healthy participants. However, people with gait disorders have a greater need for intelligent assistive devices and their anticipated locomotion when detecting obstacles should be different with the healthy. Therefore, whether the proposed strategy fits for the people with gait disorders needs to be studied. Secondly, optimizations should be employed to improve our method for practical applications. Optimization should consider the type and placement of sensors. Specifically, sensors that are simple to place, such as IMUs, can simplify the preparation for practical applications. And sensors placed on the thigh could provide more meaningful data for amputees. These considerations could guide the design of more effective assistive devices. Furthermore, while the number of stairs in the experimental platform were demonstrated enough to distinguish between transitional and steady states based on biomechanical research [4], and were adopted in previous studies [13,14,28]. However, more stairs are representative of practical applications and should be considered in future research. For optimizing machine learning methods, adaptive methods (such as Inter-Session [13], unsupervised learning [11], semi-supervised learning [43], weakly supervised learning [44] and transfer learning [45]) should be applied to a wider range of individuals without calibration or training. This can improve the usability and accessibility of assistive devices. However, there was no exploration of adaptive methods in our study. Thirdly, while SHAP algorithm provides a robust and interpretable method for comprehending complex machine learning models, it is associated with a relatively high computational cost. This limitation constrains the application of SHAP to high-dimensional data and real-time scenarios. Kernel SHAP and Tree SHAP, enhancements of the SHAP algorithm, partially address its computational costs. Kernel SHAP was employed in our study due to its model agnosticism [42]. While Tree SHAP is mainly applied to specific model types, such as decision trees and random forests. Tree SHAP demonstrates superior effectiveness, offering improved computational efficiency and reduced reliance on sampling [46]. Future research could consider exploring tree models and employing Tree SHAP for comparative analysis.

6. Conclusion

In this study, we aimed to develop a method for accurate and timely recognition of locomotion transitions. Our method employed data from the Anticipatory Locomotor Adjustment phase and removed redundant features with SHAP. It can simultaneously recognize various transition and steady-state modes with high accuracy and timeliness. The recognition accuracy reached 95.21 % with 6 channels as input, achieving a high accuracy with small data. Furthermore, increasing the input to 16 channels yielded the optimal recognition accuracy of 97.86 %. In summary, our method can accurately predict locomotion and optimize intelligent assistive devices for adapting to upcoming tasks, which is beneficial for the control of intelligent assistive devices and for the improvement of human-robot interaction. The future studies could focus on how to address limitations in locomotion prediction and adapt the

Table 3
Comparison with the state-of-the-art methods.

Reference	Locomotion	Input	Classifier	Accuracy	Highlights
Zhang et al. [11]	1 static posture & 5 steady-state modes	33 channels of sEMG, IMUs & joint angle (10 healthy participants)	MCD	source subject: 95.29 % target subject: 94.96 %	unsupervised cross-subject
Zheng et al. [13]	5 steady-state modes/ 3 steady-state modes	6 channels gyro and 6 channels acc (6 transtibial amputees)	SVM	5 modes:88.7 % 3 modes:96.6 %	inter-session & inter-day
Feng et al. [14]	5 steady-state modes/ 3 steady-state modes	ankle angle and foot pressure (3 transtibial amputees)	TCCN	5 modes:94.1 % 3 modes:96.6 %	small data driven
Narayan et al. [15]	2 static postures &7 steady-state modes	21 channels gyro and 21 channels acc (8 healthy participants)	CNN based hierarchical classifier	subject-independent: 95.87 % subject-dependent: 94.34 %	real-Time & hierarchical classification
Kang et al. [23]	5 steady-state modes/ 8 transition modes	2 channels hip angle, 6 channels gyro and 6 channels acc (20 healthy participants)	CNN	subject-independent 5 steady-state modes:98.84 % 8 transition modes:91.42 %	subject-independent
Our method	3 steady-state modes and 4 transition modes	6 channels of sEMG & gyro/ 16 channels of sEMG & gyro (10 healthy participants)	SVM	7 modes: 95.21 % (6 channels) 97.86 % (16 channels)	prediction & feature selection

mechanical parameters of intelligent assistive devices based on locomotion predictions.

CRediT authorship contribution statement

Ziyao Wang: Conceptualization, Data curation, Formal analysis, Investigation, Methodology, Resources, Software, Visualization, Writing – original draft, Writing – review & editing. **Jun Pang:** Conceptualization, Data curation, Methodology. **Pengyu Tao:** Funding acquisition, Resources, Supervision. **Zhimin Ji:** Data curation, Investigation. **Jingwen Chen:** Data curation, Methodology. **Lin Meng:** Funding acquisition, Project administration, Supervision. **Rui Xu:** Conceptualization, Funding acquisition, Project administration, Supervision, Writing – original draft, Writing – review & editing, Methodology. **Dong Ming:** Supervision, Validation.

Declaration of competing interest

The authors declare the following financial interests/personal relationships which may be considered as potential competing interests: Rui Xu reports financial support was provided by National Natural Science Foundation of China. Lin Meng reports financial support was provided by National Key Research and Development Program of China. Rui Xu reports financial support was provided by Key Laboratory of Fire Protection Technology for Industry and Public Building, Ministry of Emergency Management. If there are other authors, they declare that they have no known competing financial interests or personal relationships that could have appeared to influence the work reported in this paper.

Data availability

Data will be made available on request.

Acknowledgement

This work was supported by the National Key Research and Development Program of China (2022YFF1202500, 2022YFF1202503), the National Natural Science Foundation of China (82272115), and Key Laboratory of Fire Protection Technology for Industry and Public Building, Ministry of Emergency Management (2022KLIB09).

References

[1] J.K. Aggarwal, M.S. Ryoo, Human activity analysis, ACM Comput. Surv. 43 (2011) 1–43.
[2] P. Kumar, S. Chauhan, L.K. Awasthi, Human activity recognition (HAR) using deep learning: review, methodologies, progress and future research directions, Arch. Comput. Meth. Eng. 31 (2023) 179–219.
[3] S.W. Brose, D.J. Weber, B.A. Salatin, G.G. Grindle, H. Wang, J.J. Vazquez, R. A. Cooper, The Role of Assistive Robotics in the Lives of Persons with Disability, Am. J. Phys. Med. Rehabil. 89 (2010) 509–521.
[4] M. Grimmer, J. Zeiss, F. Weigand, G. Zhao, Joint power, joint work and lower limb muscle activity for transitions between level walking and stair ambulation at three inclinations, PLoS. One 18 (2023) e0294161.
[5] S. Chen, J. Lach, B. Lo, G.Z. Yang, Toward Pervasive Gait Analysis With Wearable Sensors: A Systematic Review, IEEE. J. Biomed. Health. Inform 20 (2016) 1521–1537.
[6] H. Prasanth, M. Caban, U. Keller, G. Courtine, A. Ijspeert, H. Vallery, J. von Zitzewitz, Wearable Sensor-Based Real-Time Gait Detection: A Systematic Review, Sensors. (basel) 21 (2021).
[7] S.Z. Homayounfar, T.L. Andrew, Wearable sensors for monitoring human motion: a review on mechanisms, materials, and challenges, SLAS. Technol 25 (2020) 9–24.
[8] H. Huang, T.A. Kuiken, R.D. Lipschutz, A strategy for identifying locomotion modes using surface electromyography, IEEE. Trans. Biomed. Eng 56 (2009) 65–73.
[9] U. Martinez-Hernandez, A.A. Dehghani-Sanij, Adaptive Bayesian inference system for recognition of walking activities and prediction of gait events using wearable sensors, Neural. Netw 102 (2018) 107–119.
[10] H. Huang, F. Zhang, L.J. Hargrove, Z. Dou, D.R. Rogers, K.B. Englehart, Continuous locomotion-mode identification for prosthetic legs based on neuromuscular-mechanical fusion, IEEE. Trans. Biomed. Eng 58 (2011) 2867–2875.
[11] K. Zhang, J. Wang, C.W. de Silva, C. Fu, Unsupervised Cross-Subject Adaptation for Predicting Human Locomotion Intent, IEEE. Trans. Neural. Syst. Rehabil. Eng. 28 (2020) 646–657.
[12] C. Cui, G.-B. Bian, Z.-G. Hou, J. Zhao, H. Zhou, A Multimodal Framework Based on Integration of Cortical and Muscular Activities for Decoding Human Intentions About Lower Limb Motions, IEEE. Trans. Biomed. Circuits. Syst. 11 (2017) 889–899.
[13] E. Zheng, Q. Wang, H. Qiao, Locomotion Mode Recognition With Robotic Transtibial Prosthesis in Inter-Session and Inter-Day Applications, IEEE. Trans. Neural. Syst. Rehabil. Eng 27 (2019) 1836–1845.
[14] Y. Feng, D. Xue, L. Ju, W. Zhang, X. Ding, Small-Data-Driven Temporal Convolutional Capsule Network for Locomotion Mode Recognition of Robotic Prostheses, IEEE. Trans. Neural. Syst. Rehabil. Eng. 30 (2022) 2540–2548.
[15] A. Narayan, F.A. Reyes, M. Ren, Y. Haoyong, Real-Time Hierarchical Classification of Time Series Data for Locomotion Mode Detection, IEEE. J. Biomed. Health. Inform 26 (2022) 1749–1760.
[16] J.D. Miller, M.S. Beazer, M.E. Hahn, Myoelectric walking mode classification for transtibial amputees, IEEE. Trans. Biomed. Eng 60 (2013) 2745–2750.
[17] A.M. Simon, K.A. Ingraham, N.P. Fey, S.B. Finucane, R.D. Lipschutz, A.J. Young, L. J. Hargrove, Configuring a powered knee and ankle prosthesis for transfemoral amputees within five specific ambulation modes, PLoS. One 9 (2014) e99387.
[18] A.J. Young, T.A. Kuiken, L.J. Hargrove, Analysis of using EMG and mechanical sensors to enhance intent recognition in powered lower limb prostheses, J. Neural. Eng 11 (2014) 056021.

[19] A.J. Young, L.J. Hargrove, A Classification Method for User-Independent Intent Recognition for Transfemoral Amputees Using Powered Lower Limb Prostheses, IEEE. Trans. Neural. Syst. Rehabil. Eng. 24 (2016) 217–225.
[20] J.A. Spanias, A.M. Simon, S.B. Finucane, E.J. Perreault, L.J. Hargrove, Online adaptive neural control of a robotic lower limb prosthesis, J. Neural. Eng 15 (2018) 016015.
[21] B.Y. Su, J. Wang, S.Q. Liu, M. Sheng, J. Jiang, K. Xiang, A CNN-Based Method for Intent Recognition Using Inertial Measurement Units and Intelligent Lower Limb Prosthesis, IEEE. Trans. Neural. Syst. Rehabil. Eng 27 (2019) 1032–1042.
[22] U.H. Lee, J. Bi, R. Patel, D. Fouhey, E. Rouse, Image Transformation and CNNs: A Strategy for Encoding Human Locomotor Intent for Autonomous Wearable Robots, IEEE. Rob. Autom. Lett. 5 (2020) 5440–5447.
[23] I. Kang, D.D. Molinaro, G. Choi, J. Camargo, A.J. Young, Subject-Independent Continuous Locomotion Mode Classification for Robotic Hip Exoskeleton Applications, IEEE. Trans. Biomed. Eng 69 (2022) 3234–3242.
[24] R.C. Sheehan, J.S. Gottschall, Stair walking transitions are an anticipation of the next stride, J. Electromyogr. Kinesiol 21 (2011) 533–541.
[25] L. Alcock, T.D. O'Brien, N. Vanicek, Biomechanical demands differentiate transitioning vs. continuous stair ascent gait in older women, Clin. Biomech. (Bristol, Avon), 29 (2014) 111-118.
[26] L. Alcock, T.D. O'Brien, N. Vanicek, Biomechanical demands of the 2-step transitional gait cycles linking level gait and stair descent gait in older women, J. Biomech. 48 (2015) 4191–4197.
[27] B. Chen, E. Zheng, Q. Wang, A locomotion intent prediction system based on multi-sensor fusion, Sensors. (basel) 14 (2014) 12349–12369.
[28] D. Xu, Y. Feng, J. Mai, Q. Wang, Real-Time On-Board Recognition of Continuous Locomotion Modes for Amputees With Robotic Transtibial Prostheses, IEEE. Trans. Neural. Syst. Rehabil. Eng 26 (2018) 2015–2025.
[29] L. Meng, J. Pang, Z. Wang, R. Xu, D. Ming, The Role of Surface Electromyography in Data Fusion with Inertial Sensors to Enhance Locomotion Recognition and Prediction, Sensors. (basel) 21 (2021).
[30] S. Rietdyk, Anticipatory locomotor adjustments of the trail limb during surface accommodation, Gait. Posture 23 (2006) 268–272.
[31] J. Peng, N.P. Fey, T.A. Kuiken, L.J. Hargrove, Anticipatory kinematics and muscle activity preceding transitions from level-ground walking to stair ascent and descent, J. Biomech 49 (2016) 528–536.
[32] A.H. Al-Timemy, G. Bugmann, J. Escudero, N. Outram, Classification of finger movements for the dexterous hand prosthesis control with surface electromyography, IEEE. J. Biomed. Health. Inform 17 (2013) 608–618.
[33] S.M. Lundberg, S.-I. Lee, A unified approach to interpreting model predictions, Proceedings of the 31st International Conference on Neural Information Processing Systems, Curran Associates Inc., Long Beach, California, USA, 2017, pp. 4768–4777.
[34] S.M. Lundberg, B. Nair, M.S. Vavilala, M. Horibe, M.J. Eisses, T. Adams, D. E. Liston, D.K. Low, S.F. Newman, J. Kim, S.I. Lee, Explainable machine-learning predictions for the prevention of hypoxaemia during surgery, Nat. Biomed. Eng 2 (2018) 749–760.
[35] S.M. Lauritsen, M. Kristensen, M.V. Olsen, M.S. Larsen, K.M. Lauritsen, M. J. Jorgensen, J. Lange, B. Thiesson, Explainable artificial intelligence model to predict acute critical illness from electronic health records, Nat. Commun 11 (2020) 3852.
[36] X. Song, A.S.L. Yu, J.A. Kellum, L.R. Waitman, M.E. Matheny, S.Q. Simpson, Y. Hu, M. Liu, Cross-site transportability of an explainable artificial intelligence model for acute kidney injury prediction, Nat. Commun 11 (2020) 5668.
[37] N. Gozzi, L. Malandri, F. Mercorio, A. Pedrocchi, XAI for myo-controlled prosthesis: Explaining EMG data for hand gesture classification, Knowl.-Based. Syst. 240 (2022).
[38] Y. Liu, Z. Liu, X. Luo, H. Zhao, Diagnosis of Parkinson's disease based on SHAP value feature selection, Biocybernetics and Biomedical, Engineering 42 (2022) 856–869.
[39] J. Hancock, R. Bauder, T.M. Khoshgoftaar, A Model-Agnostic Feature Selection Technique to Improve the Performance of One-Class Classifiers, 2023 IEEE 35th International Conference on Tools with Artificial Intelligence (ICTAI), 2023, pp. 92-98.
[40] A. Phinyomark, P. Phukpattaranont, C. Limsakul, Feature reduction and selection for EMG signal classification, Expert. Syst. Appl. 39 (2012) 7420–7431.
[41] A. Phinyomark, F. Quaine, S. Charbonnier, C. Serviere, F. Tarpin-Bernard, Y. Laurillau, EMG feature evaluation for improving myoelectric pattern recognition robustness, Expert. Syst. Appl. 40 (2013) 4832–4840.
[42] K. Aas, M. Jullum, A. Løland, Explaining individual predictions when features are dependent: More accurate approximations to Shapley values, Artif. Intell. 298 (2021).
[43] Z. Ren, X. Kong, Y. Zhang, S. Wang, UKSSL: underlying knowledge based semi-supervised learning for medical image classification, IEEE Open. J. Eng. Med. Biol. (2023) 1–8.
[44] Z. Ren, S. Wang, Y. Zhang, Weakly supervised machine learning, CAAI Trans. Intelligence. Technol. 8 (2023) 549–580.
[45] Y. Zhang, L. Deng, H. Zhu, W. Wang, Z. Ren, Q. Zhou, S. Lu, S. Sun, Z. Zhu, J. M. Gorriz, S. Wang, Deep learning in food category recognition, Information. Fusion 98 (2023).
[46] S.M. Lundberg, G. Erion, H. Chen, A. DeGrave, J.M. Prutkin, B. Nair, R. Katz, J. Himmelfarb, N. Bansal, S.I. Lee, From local explanations to global understanding with explainable AI for trees, Nat. Mach. Intell 2 (2020) 56–67.